Supporting Information for Ultra-Sensitive Broadband Probing of Molecular Vibrational Modes with Multifrequency Optical Antennas

Heykel Aouani,[*,†] Hana Sipova,[‡] Mohsen Rahmani,[¶,§] Miguel Navarro-Cia,[‖,⊥] Katerina Hegnerova,[‡] Jiri Homola,[‡] Minghui Hong,[§] and Stefan A. Maier[†]

[†] *The Blackett Laboratory, Department of Physics, Imperial College London, London SW7 2AZ, United Kingdom,* [‡] *Institute of Photonics and Electronics, Academy of Sciences of the Czech Republic, Chaberska 57, 18251 Prague, Czech Republic,* [¶] *Data Storage Institute, (A*STAR) Agency for Science, Technology and Research, 5 Engineering Drive 1, Singapore 117608,* [§] *Department of Electrical and Computer Engineering, National University of Singapore, Singapore 117576,* [‖] *Department of Electronic & Electrical Engineering, University College London, London WC1E 7JE, United Kingdom, and* [⊥] *Optical and Semiconductor Devices Group, Department of Electrical and Electronic Engineering, Imperial College London, London SW7 2BT, United Kingdom*

E-mail: h.aouani@imperial.ac.uk

[*]To whom correspondence should be addressed
[†]Imperial College, The Blackett Laboratory
[‡]Acad Sci Czech Republic
[¶]A*STAR
[§]National University of Singapore
[‖]University College London
[⊥]Imperial College, Optical and Semiconductor Devices Group

We present in Figure S1a a set of simulations showing the simulated absorption, scattering and extinction cross sections of the multifrequency trapezoidal nanoantenna. The charge density distribution at the plane of the middle cross section of the nanoantenna is respectively plotted in Figure S1b,c for resonance peaks at 1370 cm^{-1} (7300 nm) and 1923 cm^{-1} (5200 nm). We notice in Figure S1b,c how different pairs of opposite neighboring teeth are active at each resonance in a dipolar fashion. As the wavenumber shifts from shorter to longer values, the pair of teeth excited move from the outermost to the innermost ones. These pairs of local-induced dipoles oriented almost parallel to the incoming polarization intercept the incoming wave and the captured energy is guided to the vertices, creating an extremely confined vertical dipole at the gap responsible for the intensity enhancement shown in Figure S1d,e of the main document.

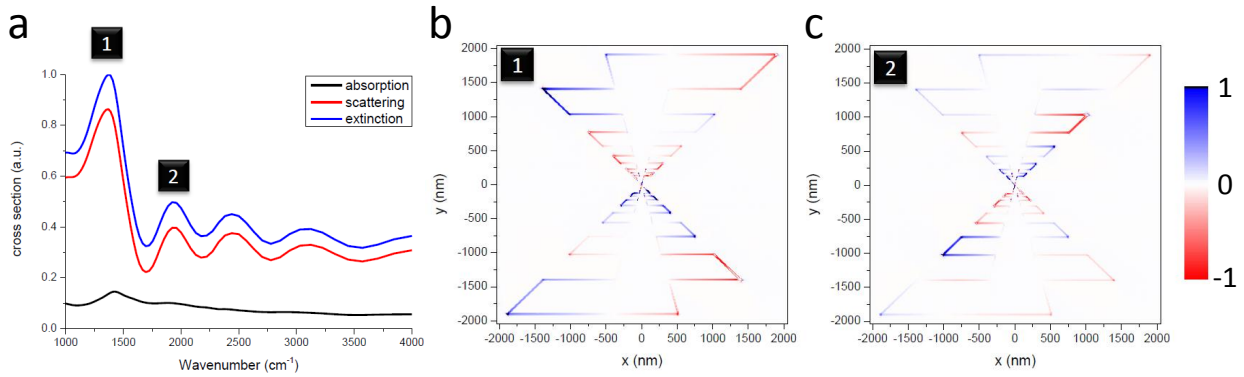

Figure S1: (a) Simulated absorption (black line), scattering (red line) and extinction (blue line) cross sections of the multifrequency optical antenna. Charge density distribution at the plane of the middle cross section for resonance peaks at 1370 cm^{-1} (b) and 1923 cm^{-1} (c).

To determine the electric field enhancement provided by the multifrequency optical antenna, we illuminated it from the semi-infinite air space with a x-polarized plane-wave propagating along z. The electromagnetic field enhancement (defined as $|E(x,y)|^2/|E_0|^2$) at the plane of the middle cross section is displayed in Figure S2a for the four resonance peaks (1370 cm^{-1}, 1923 cm^{-1}, 2439 cm^{-1} and 3226 cm^{-1}) indicated in Figure S2b. As we can see, a high electromagnetic enhancement is generated in the vicinity of the multifrequency optical antenna on a bandwidth of several octaves. Numerical simulation of the intensity enhancement on a reference flat gold film (thickness 60 nm) is also presented in Figure S2c.

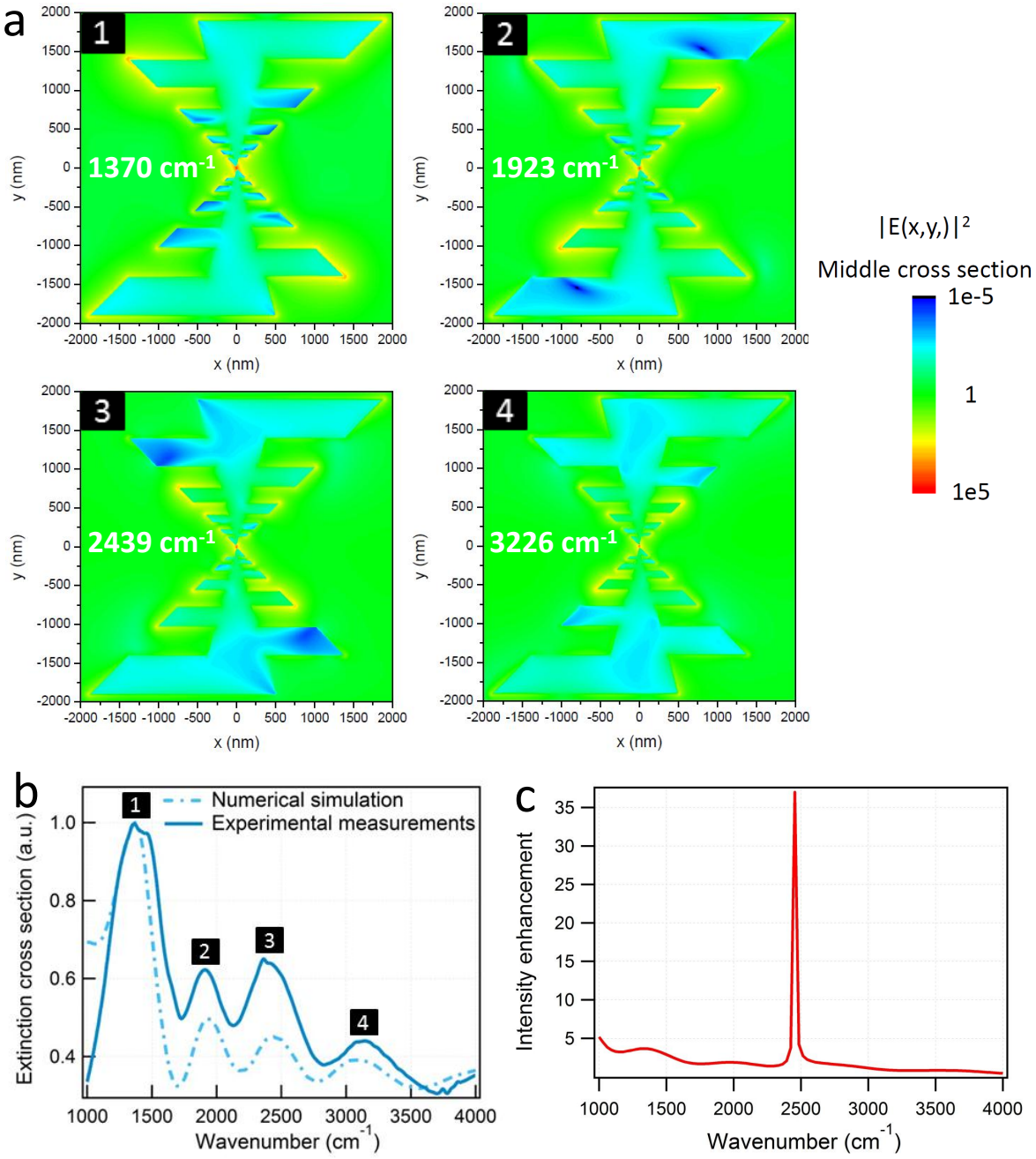

Figure S2: (a) Extinction cross section of the trapezoidal nanoantenna presented in Figure 1c. The four resonance peaks are numbered from the fundamental (1) to the fourth resonance (4).(b) Intensity enhancement of the electric field with respect to the incident field ($|E(x,y)|^2$ / $|E_0|^2$) provided by the multifrequency optical antenna at the plane of the middle cross section for the four resonance peaks at 1370 cm^{-1}, 1923 cm^{-1}, 2439 cm^{-1} and 3226 cm^{-1}. (c) Intensity enhancement at the surface of a 60 nm gold film when illuminated by a plane-wave (TM polarized) under grazing incidence (80°).

A SEM image with high magnification at the gap of the fabricated trapezoidal nanoantenna is available in Figure S3a. From this SEM image, the gap was estimated to 20 nm, in agreement with our numerical simulations. A 3D AFM image of the nanostructure is also presented in Figure S3b.

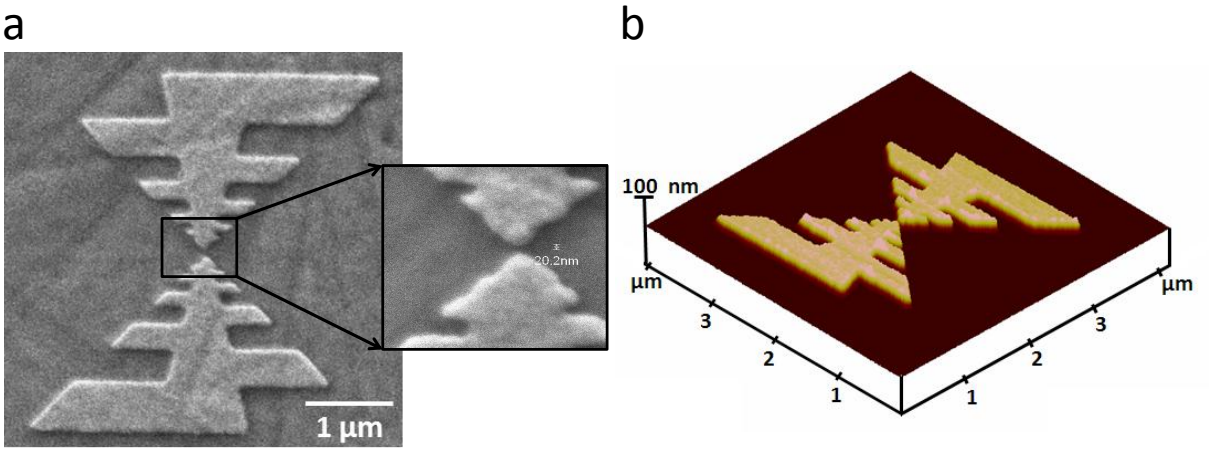

Figure S3: (a) SEM image with high magnification at the gap and (b) 3D AFM image of the fabricated trapezoidal optical antenna.

Schematic representations of self-assembled monolayer (SAM) of carboxy-terminated alkanethiols adsorbed on trapezoidal optical antennas are presented in Figure S4a,b, respectively corresponding to configurations before and after treatment of EDC and NHS mixture.

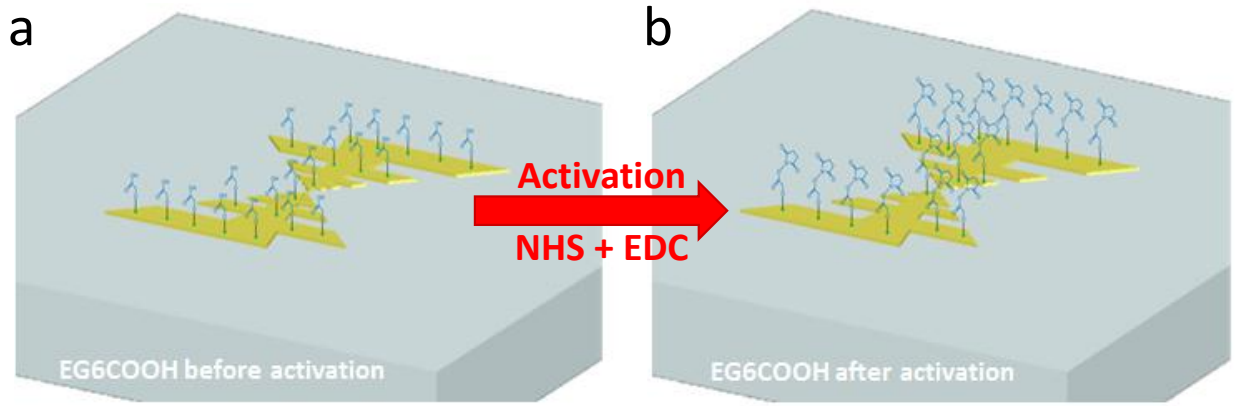

Figure S4: Schematic representation of alkanethiol adsorption on multifrequency optical antennas before (a) and after (b) treatment with EDC and NHS mixture.

Finally, Figure S5 displays an example of experimental raw extinction spectrum measured in the case of AT-EG−6-COOH adsorbed on a flat gold film (a) and on an optical antenna array (b). The spot size used for the reference measurements on the flat gold film is elliptical (2.5 mm × 20 mm).

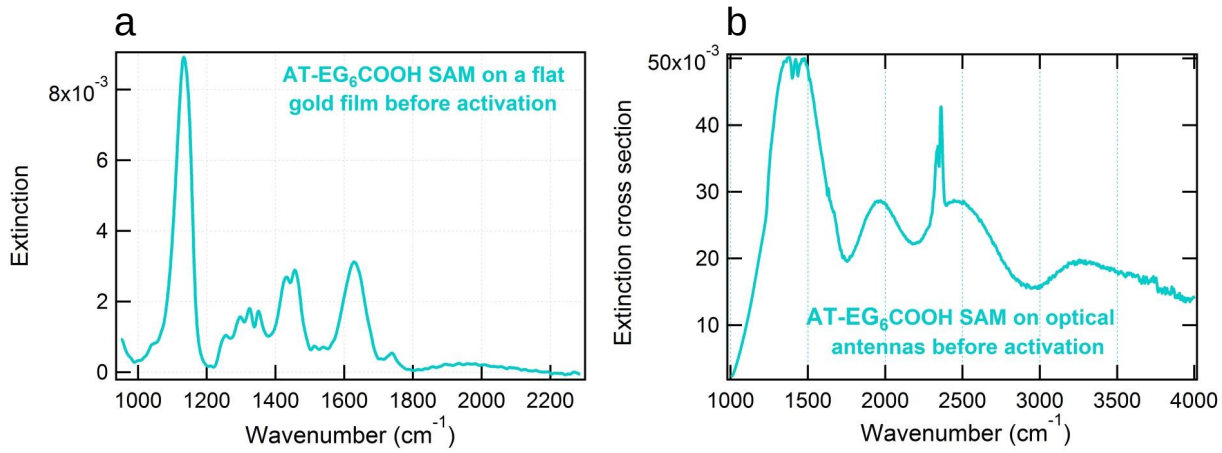

Figure S5: Infrared extinction spectrum of alkanethiol molecule before treatment of EDC and NHS mixture measured in the case of adsorption on a flat gold film under grazing illumination (a) and on trapezoidal nanoantenna array (b).